Supporting Information

Dopant Distributions and Band-Edge Positions in Sr-Doped $NaTaO_3$: A First-Principles Study

Ryusei Morimoto[1], Hiroki Uratani[1,2,], Hiroshi Onishi[3,4,5], Hirofumi Sato[1,6]*

[1]Department of Molecular Engineering, Graduate school of Engineering, Kyoto University, Nishikyo-ku, Kyoto 615-8510, Japan

[2] PRESTO, Japan Science and Technology Agency (JST), Kawaguchi, Saitama 332-0012, Japan

[3] Department of Chemistry, Graduate School of Science, Kobe University, Nada-ku, Kobe 657-8501, Japan

[4] Research Center for Membrane and Film Technology, Kobe University, Nada-ku, Kobe 657-8501, Japan

[5] Division of Advanced Molecular Science, Institute for Molecular Science, Okazaki 444-8585, Japan

[6] Fukui Institute for Fundamental Chemistry, Kyoto University, Sakyo-ku, Kyoto 606-8103, Japan

Details of structure enumeration

Prior to Sr substitution, the fractional coordinates of Na and Ta in the relaxed $NaTaO_3$ unit cell were slightly regularized to minimize spurious symmetry breaking and thereby reduce the number of generated structures. After unit-cell optimization, small deviations from ideal fractional positions can lower the space-group symmetry; we therefore snapped near-symmetric coordinates to their ideal values (e.g., (x, y, z) = (0.004, 0.003, 0.2500) → (0.000, 0.000, 0.2500)). The magnitude of these corrections was < 0.03 in fractional (0–1) units for any coordinate.

Using the symmetry-regularized cell, we then generated candidate doped structures by selecting three Na sites and one Ta site (3Na1Ta scheme). To avoid redundant calculations, symmetrically equivalent configurations were merged (i.e., only one representative per equivalence class was retained). In determining equivalence, we considered the cation sublattice (Na/Ta/Sr) and ignored oxygen positions which do not affect the enumeration of Sr placements on A/B sites.

Details of spin polarization.

Spin polarized DFT calculations were performed for NTO and for two representative B2-3Na1Ta configurations, denoted B2-3Na1Ta(I) and B2-3Na1Ta(II). B2-3Na1Ta (I) has the shortest Sr-Sr distance among all B2-3Na1Ta configurations, whereas B2-3Na1Ta(II) has the longest Sr-Sr distance. All structures were first optimised using non-spin polarized DFT, and spin polarization was then included for the optimised geometries.

For B2-3Na1Ta(I), the total magnetic moment remained 0.000 μ_B when spin-polarization was included. For B2-3Na1Ta(II), a finite magnetic moment of 0.396 μ_B was obtained; however the energy difference between spin-polarized and non-spin polarized calculations was small (0.015 eV). Because the energetically most stable configurations in our dataset correspond to shorter Sr-Sr distances, we conclude that spin polarization has a negligible effect on the relative stabilities and the key electronic-structure trends discussed in this work.

Table S1. Total magnetic moments (μ_B) and relative energies (eV) for bulk NTO and B2-3Na1Ta. B2-3Na1Ta(I) has the shortest Sr-Sr distance among all B2-3Na1Ta configurations, whereas B2-3Na1Ta(II) has the longest.

Model	Method	M_{tot} (μ_B)	ΔE (eV)
Bulk NTO	Non-spin polarized	-	0.000
	Spin polarized	0.000	0.000
B2-3Na1Ta(I)	Non-spin polarized	-	0.000
	Spin polarized	0.000	0.000
B2-3Na1Ta(II)	Non-spin polarized	-	0.737
	Spin polarized	0.396	0.722

Supporting figures and tables

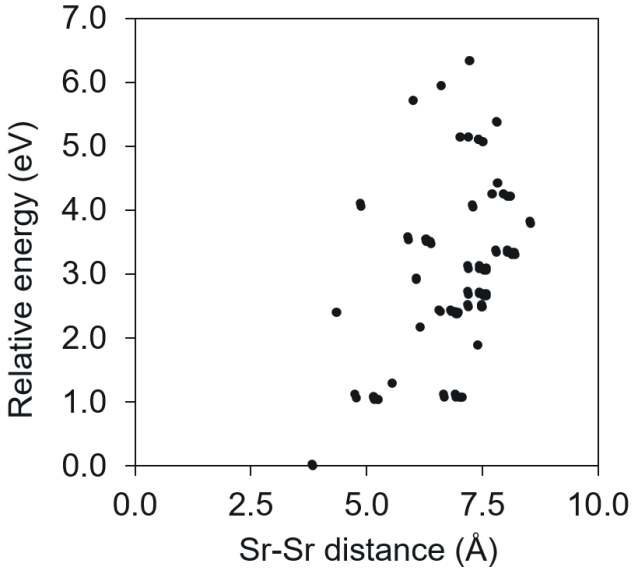

Figure S1. Sr-Sr distance dependence of relative energy for **B1-3Na1Ta**.

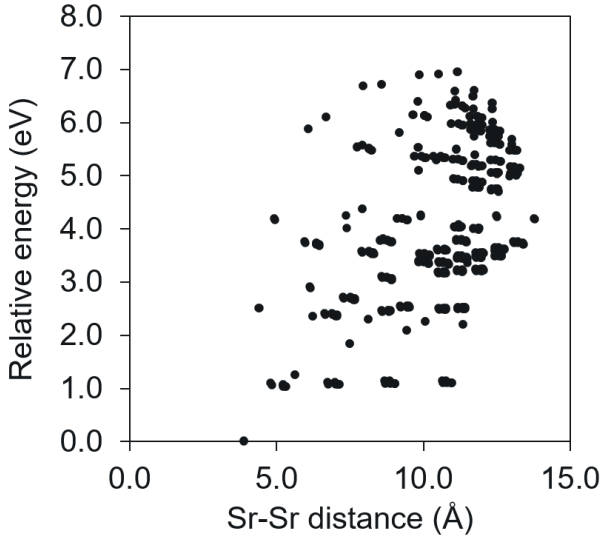

Figure S2. Sr-Sr distance dependence of relative energy for **B2-3Na1Ta** .

Table S2. Structure parameters of bulk NTO and **3Na1Ta** models.

Model	Sr (mol%/Ta)	V (Å^3)	ΔV%	a (Å)	b (Å)	c (Å)
Bulk NTO	0	233.8	0	5.45	5.52	7.77
B1-3Na1Ta	36.4	245.1	4.8	5.51	5.58	7.98
B2-3Na1Ta	21.1	242.3	3.6	5.49	5.56	7.93
B3-3Na1Ta	12.9	239.5	2.4	5.50	5.56	7.83
B4-3Na1Ta	5.1	235.2	0.6	5.46	5.53	7.79
Expt.[1]	0	235.5	0.7	5.48	5.52	7.79
Expt.[2]	8.0	237.8	1.7	5.55	5.50	7.79

Table S3. Structure parameters of relaxed bulk NTO and **B3** models.

Composition	Sr (mol%/Ta)	V (nm^3)	ΔV%	a (Å)	b (Å)	c (Å)
Bulk NTO	0	233.8	0	5.45	5.52	7.77
B3-1Na	3.1	234.7	0.4	5.46	5.52	7.79
B3-1Na-c	3.1	233.6	−0.1	5.45	5.52	7.77
B3-1Ta	3.2	235.9	0.9	5.46	5.54	7.79
B3-1Ta-c	3.2	238.0	1.8	5.48	5.56	7.81
B3-3Na1Ta	12.9	239.5	2.4	5.50	5.56	7.83

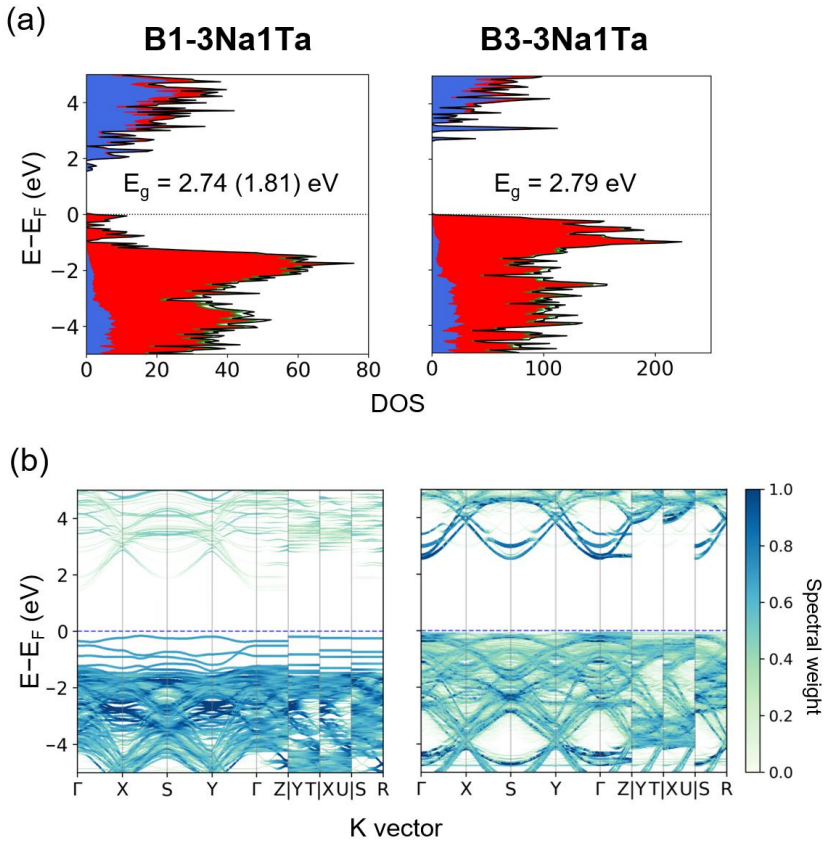

Figure S3. (a) PDOS for **B1-3Na1Ta** and **B3-3Na1Ta**. Total DOS (black), Ta (blue), O (red), Sr (green); energies referenced to fermi energy. (b) Unfolded band structures, where the color indicates the spectral weight.

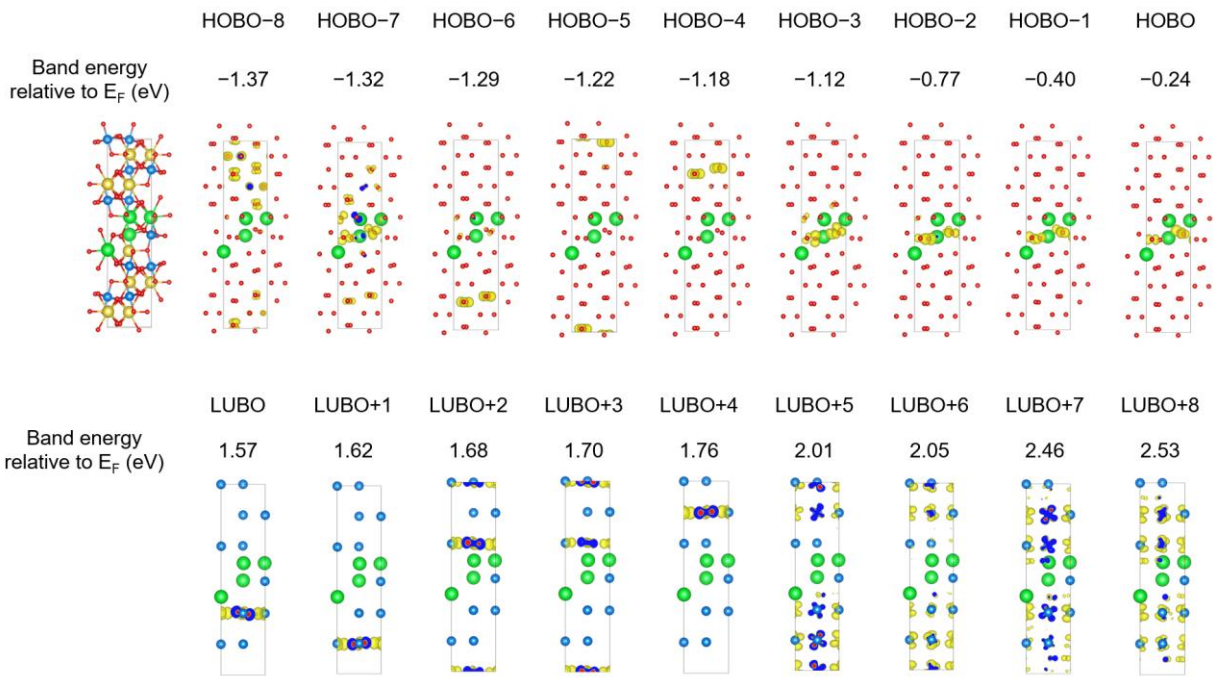

Figure S4. Charge density distributions of **B1-3Na1Ta**. HOBO: highest occupied band orbital; LUBO: lowest unoccupied band orbital.

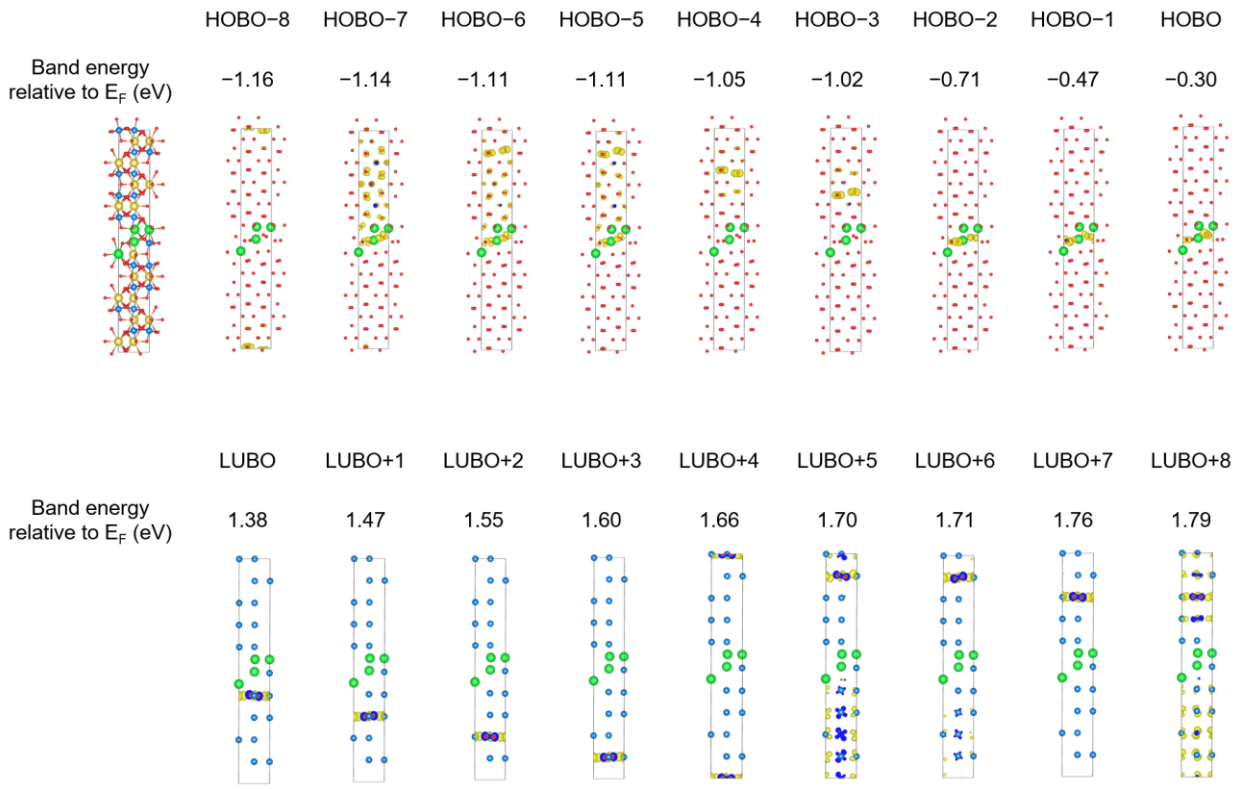

Figure S5. Charge density distributions of **B2-3Na1Ta**. HOBO: highest occupied band orbital; LUBO: lowest unoccupied band orbital.

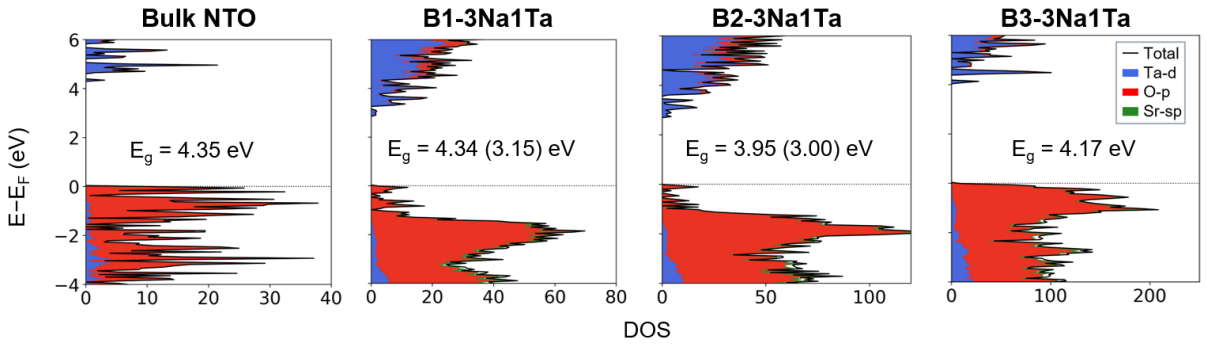

Figure S6. PDOS for bulk NTO, B1-3Na1Ta, B2-3Na1Ta, and B3-3Na1Ta computed using HSE06. Total DOS (black line), Ta (blue), O (red), Sr (green); energies referenced to fermi energy.

Table S4. Bader charges for unrelaxed **B2-3Na1Ta**. 3Na1Ta (I) has the shortest Sr-Sr distance in the enumeration and (II) is the longest one.

Structure	Distance between Sr(Ta) and Sr(Na) layers (Å)	Bader charges			
		O near Sr(Ta)	O near Sr(Na)	Sr(Ta)	Sr(Na)
NTO (bulk)		−1.29	−1.29		
3Na1Ta (I)	3.9	−1.28	−1.28	+1.49	+1.55
3Na1Ta (II)	13.8	−1.05	−1.33	+1.54	+1.55

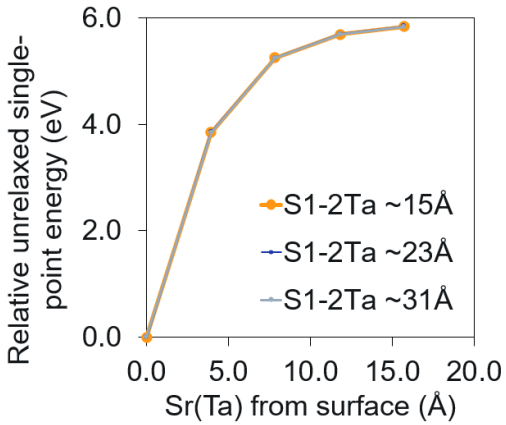

Figure S7. Relative energies of **S1-2Ta** configurations with respect to Sr distance from the top surface.

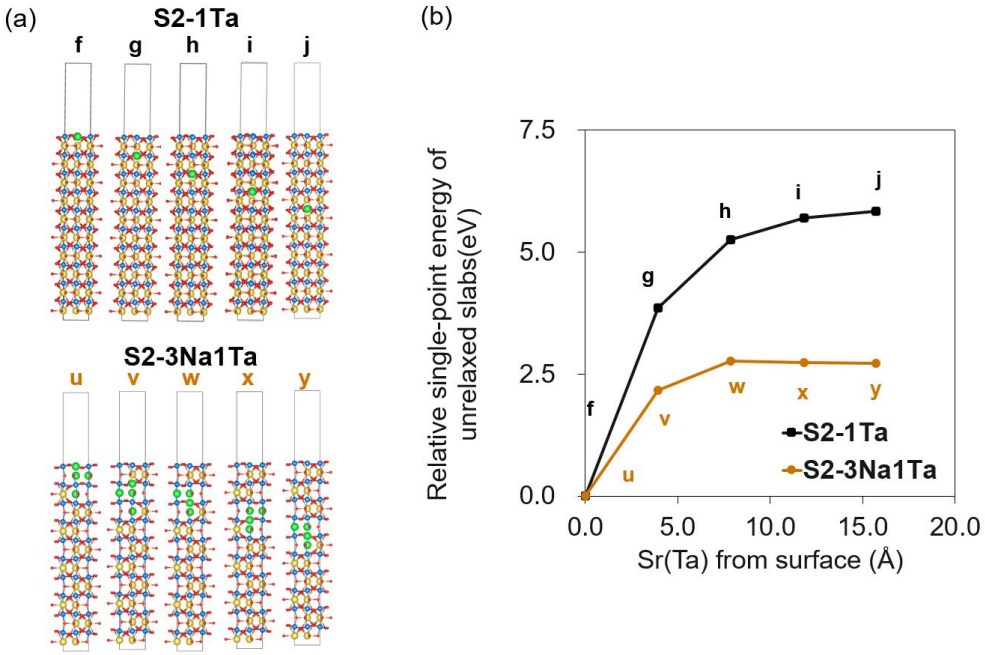

Figure S8. (a) **S2-1Ta** (**f-j**) and **S2-3Na1Ta** (**u-y**) models. (b) Sr distance from surface dependence of relative energy for **S2-1Ta** and **S2-3Na1Ta** models.

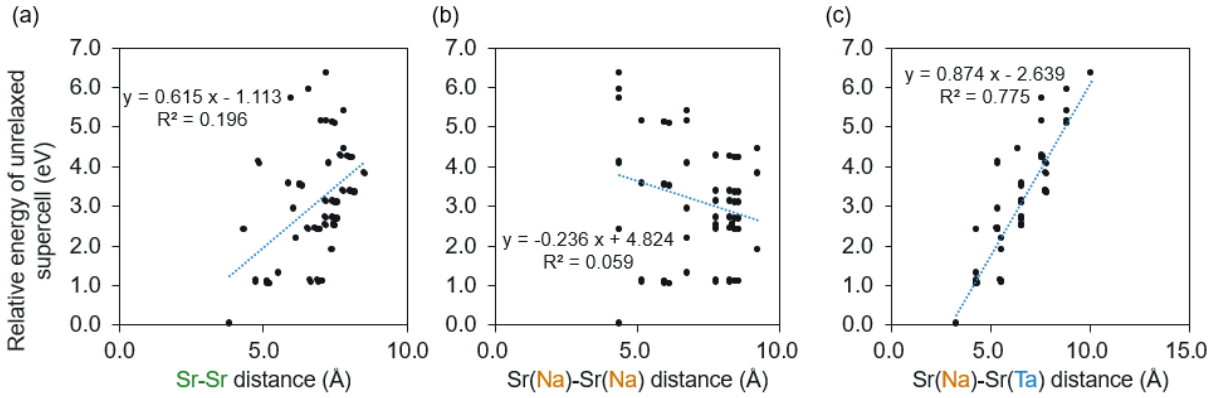

Figure S9. Sr–Sr distance dependence of relative energy for **B1-3Na1Ta**. Relative single-point energy of unrelaxed configurations plotted against the mean pair separation (Å). (a) all Sr–Sr pairs; (b) Sr(Na)–Sr(Na) pairs; (c) Sr(Na)–Sr(Ta) pairs. Dashed lines are least-squares linear fits; slope and R^2 are shown in each panel.

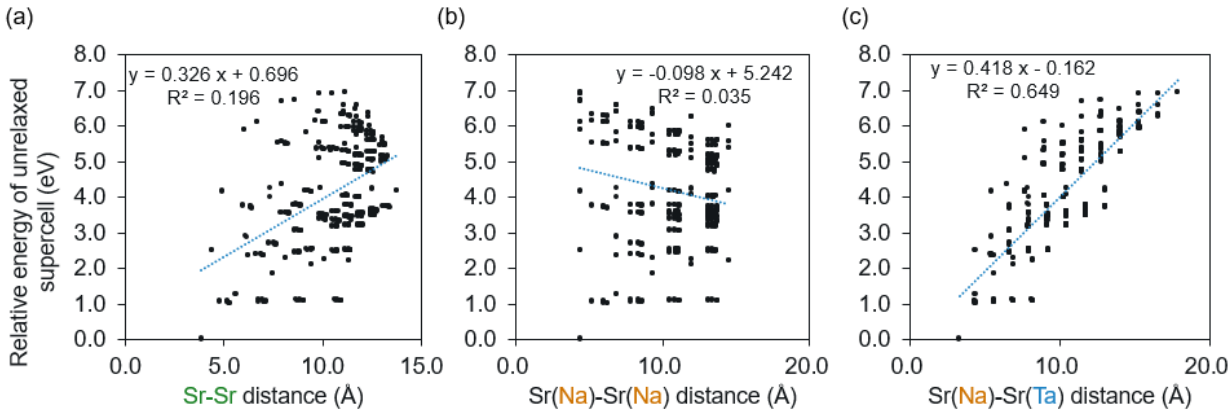

Figure S10. Sr–Sr distance dependence of relative energy for **B2-3Na1Ta**. Relative single-point energy of unrelaxed configurations plotted against the mean pair separation (Å). (a) all Sr–Sr pairs; (b) Sr(Na)–Sr(Na) pairs; (c) Sr(Na)–Sr(Ta) pairs. Dashed lines are least-squares linear fits; slope and R^2 are shown in each panel.

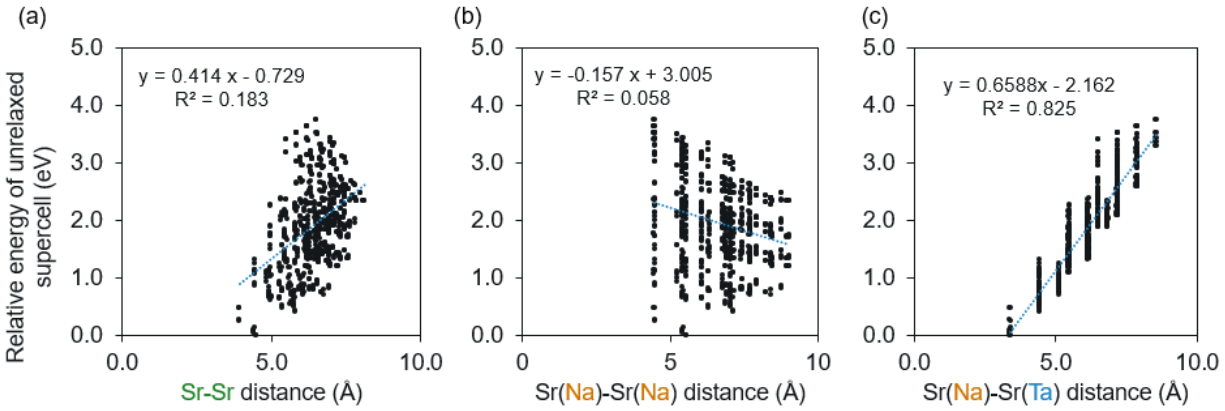

Figure S11. Sr–Sr distance dependence of relative energy for **B3-3Na1Ta**. Relative single-point energy of unrelaxed configurations plotted against the mean pair separation (Å). (a) all Sr–Sr pairs; (b) Sr(Na)–Sr(Na) pairs; (c) Sr(Na)–Sr(Ta) pairs. Dashed lines are least-squares linear fits; slope and R^2 are shown in each panel.

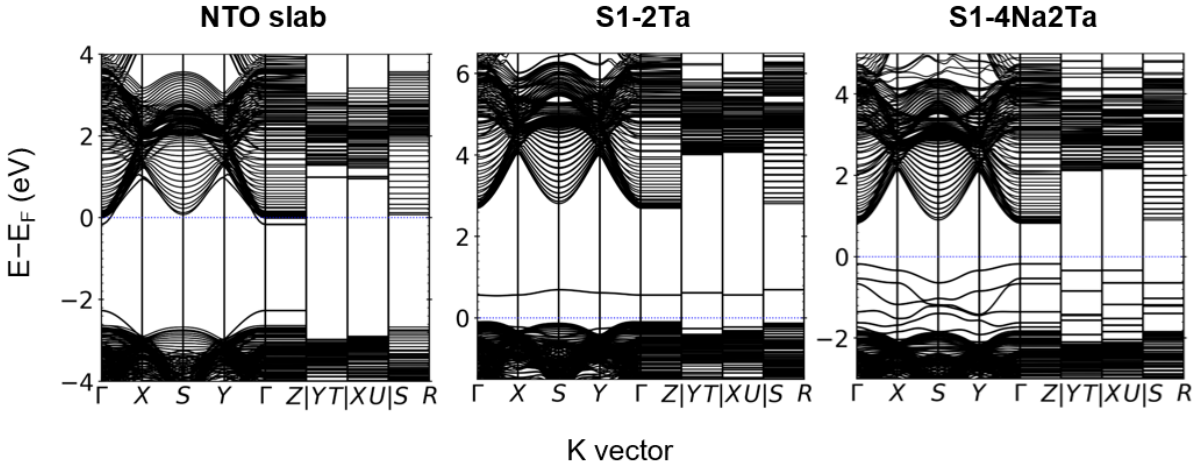

Figure S12. Electronic band structures for surface slab models.

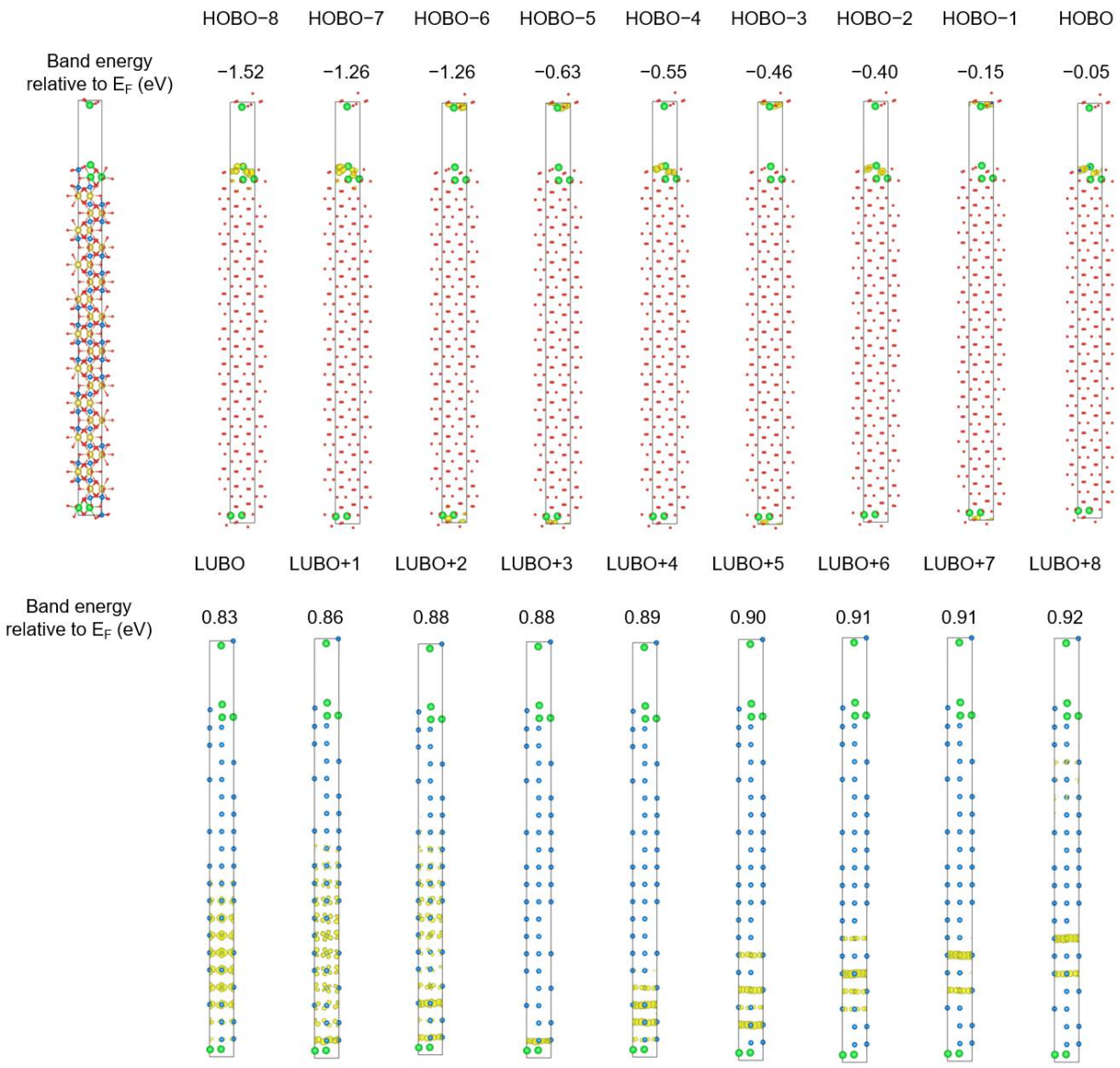

Figure S13. Charge density distributions of **S1-4Na2Ta** model. HOBO: highest occupied band orbital; LUBO: lowest unoccupied band orbital.

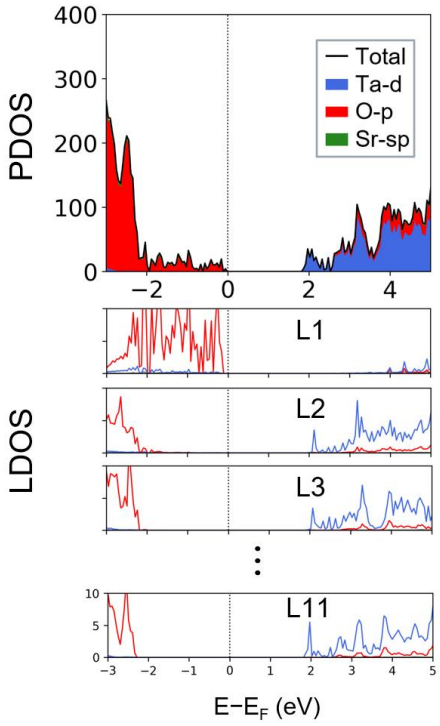

Figure S14. PDOS and LDOS for S1-4Na2Ta calculated using HSE06. Energies are referenced to the Fermi energy, with E_F = 0 eV. L1 denotes the surface layer, and L11 denotes the bulk-like interior (farthest from the surface).

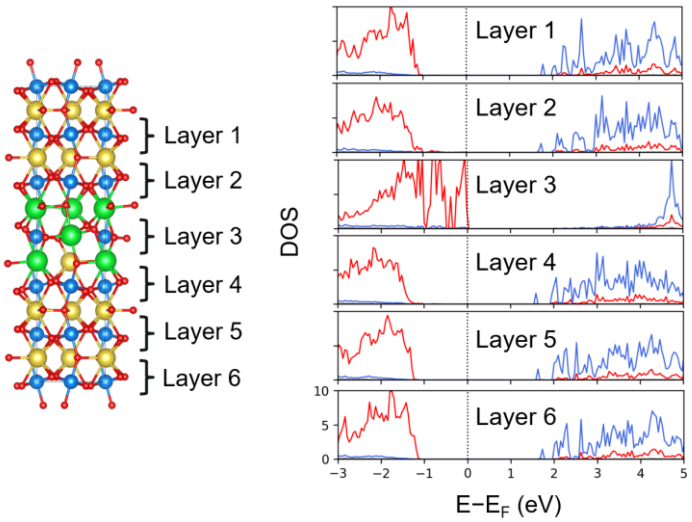

Figure S15. Layer-resolved LDOS for **B1-3Na1Ta**.

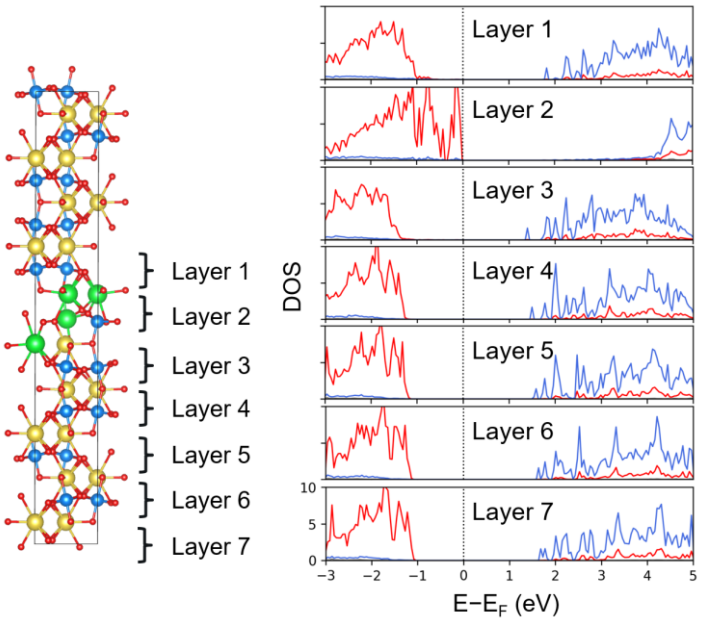

Figure S16. Layer-resolved LDOS for **B2-3Na1Ta**.

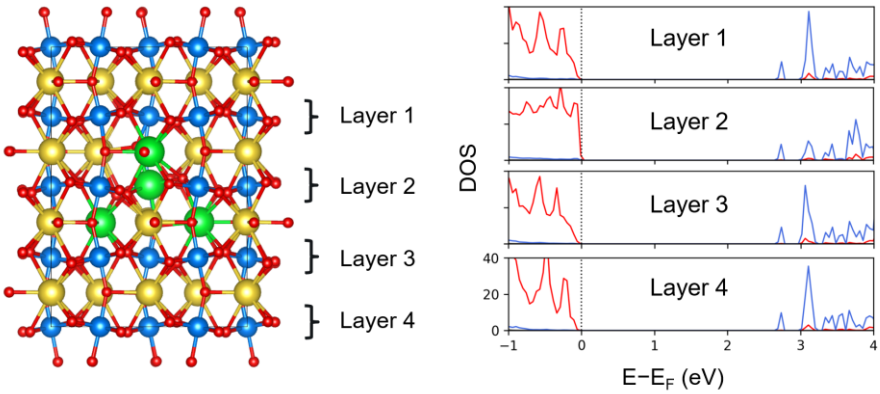

Figure S17. Layer-resolved LDOS for **B3-3Na1Ta**.

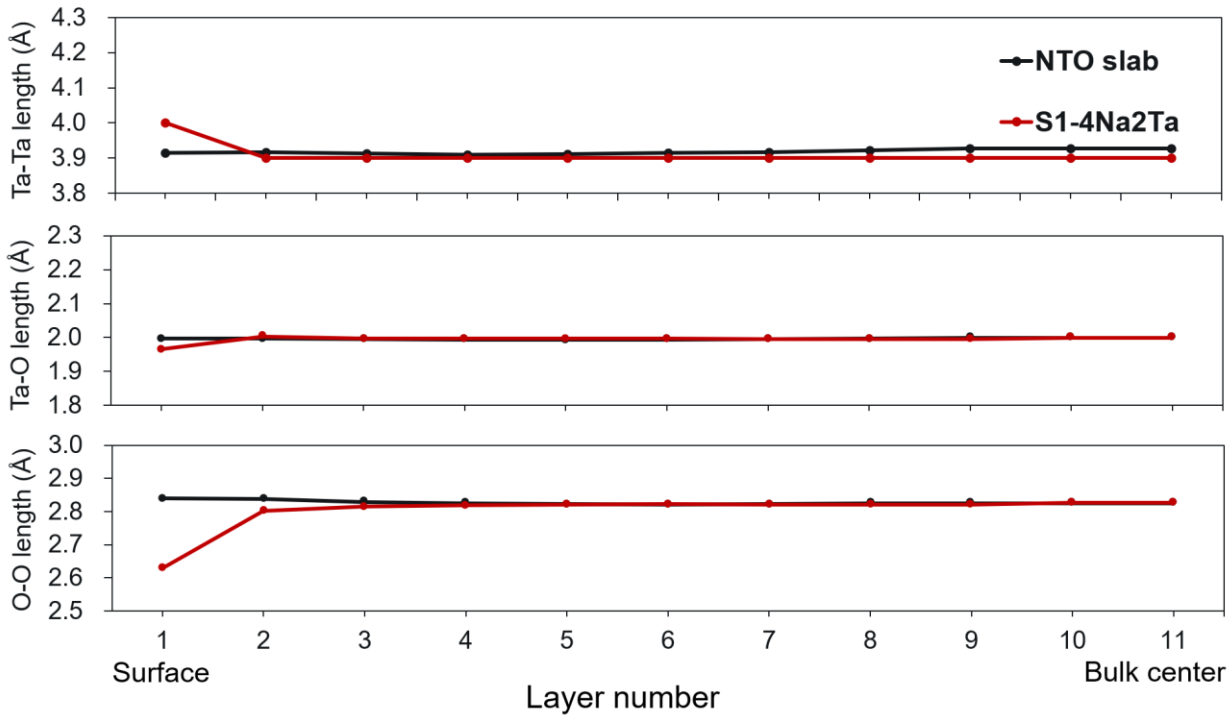

Figure S18. Layer-resolved bond length for surface slabs.

Supporting references

(1) Kennedy, B. J.; Prodjosantoso, A. K.; Howard, C. J. Powder Neutron Diffraction Study of the High Temperature Phase Transitions in NaTaO3. *J. Phys. Condens. Matter* **1999**, *11* (33), 6319. https://doi.org/10.1088/0953-8984/11/33/302.

(2) An, L.; Sasaki, T.; Weidler, P. G.; Wöll, C.; Ichikuni, N.; Onishi, H. Local Environment of Strontium Cations Activating NaTaO3 Photocatalysts. *ACS Catal.* **2018**, *8* (2), 880–885. https://doi.org/10.1021/acscatal.7b03567.